

## NEW POWER OPTIMIZATION POSSIBILITIES OF STATIC CONVERTER AND ASYNCHRONOUS MOTOR DRIVING SYSTEMS

Alexandru BITOLEANU, Mihaela POPESCU

*Electric Drives and Power Electronics Department, Faculty for Electromechanical  
Engineering, University of Craiova, Romania*

Abstract: In this paper there are given a few mathematical relations for the power analysis in un-sinusoidal regime. If the voltage is sinusoidal and the current is un-sinusoidal, the apparent power will be ascertained by the active power, the fundamental displacement factor and on the current distortion factor. If the voltage and the current are un-sinusoidal, there will exist the optimum values for real parts of harmonics impedances that will minimize the apparent power. More interesting is the possibility of minimization the apparent power at constant mechanical power.

Keywords: nonsinusoidal regime, distortion power, optimal control.

### 1. INTRODUCTION

Voltage and frequency static converters are producing un-sinusoidal regime sources and, in the same time, loads. So, they influence the network because they consume an un-sinusoidal current, but they influence the ac motor (asynchronous or synchronous) through the voltage or the current provided. The improvement of the driving systems with these converters requires a power approach of their function.

If the voltage is sinusoidal and the current is un-sinusoidal, the apparent power will be dependent on the active power, the fundamental displacement factor and on the current distortion factor (Bitoleanu A., M. Popescu 2000). The input fundamental power factor (FPF) of PWM converters and ac motors driving systems is usually nearly unit. But the total power factor (TPF) depends on the modulation strategy and the filter by DC link voltage circuit (Bitoleanu, A., M. Popescu 1998).

### 2. THE STRUCTURE OF THE DRIVING SYSTEM

The structure of the driving system with asynchronous motor and frequency static converters with dc link circuit that has the characteristic of a voltage source is shown in fig. 1. The L-C filter in the dc link circuit separates the inverter from the rectifier, respectively from the network. So, it is very likely that the power performances within the network will be influenced in a qualitative way by the components of the filter and only in a quantitative way by the current required by the inverter (Bitoleanu A., M. Popescu 2001).

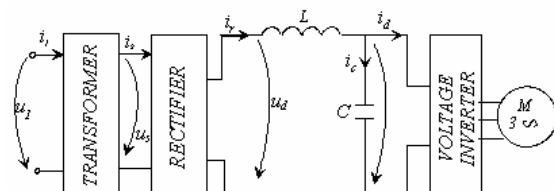


Fig. 1 The structure of the driving system

3. THE LINK BETWEEN THE NETWORK  
AND THE STATIC CONVERTER

3.1. The mathematical characterization

If the network is strong enough, its voltage will be practically sinusoidal

$$(1) u(t) = \sqrt{2}U \sin \omega t.$$

The current  $i_s$  is  $\pm i_r$  (Fig. 2) and it is un-sinusoidal, but its average value is zero

$$(2) i(t) = \sqrt{2} \sum_{k=1}^{\infty} I_k \sin(k\omega t - \varphi_k).$$

The active power is on fundamental only

$$(3) P = UI_1 \cos \varphi_1.$$

The apparent power is

$$(4) S = UI = U \sqrt{\sum_{k=1}^{\infty} I_k^2} = UI_1 \sqrt{1 + \sum_{k=2}^{\infty} \left(\frac{I_k}{I_1}\right)^2} \\ = UI_1 \sqrt{1 + FDI^2}$$

The active power is imposed by the electrical motor, so, from (3) there is obtained

$$I_1 = \frac{P}{U \cos \varphi_1} \text{ and the apparent power is}$$

$$(5) S = \frac{P}{\cos \varphi_1} \sqrt{1 + FDI^2}.$$

So, the global power factor will be

$$(6) TPF = \frac{\cos \varphi_1}{\sqrt{1 + FDI^2}}.$$

Budeanu's reactive power is (Budeanu C.I. 1936).

$$(7) Q_B = UI_1 \sin \varphi_1 = P \tan \varphi_1.$$

Czarnecki's reactive power is (Czarnecki L.S. 1985)

$$Q_C = U \sum_{k=1}^{\infty} I_k \sin \varphi_k = Q_B \left( 1 + \sum_{k=2}^{\infty} \frac{I_k}{I_1} \frac{\sin \varphi_k}{\sin \varphi_1} \right)$$

Budeanu's distortion power has the expression

$$(9) D_B = \sqrt{S^2 - P^2 - Q_B^2} = S \frac{FDI}{\sqrt{1 + FDI^2}} \\ = \frac{P}{\cos \varphi_1} FDI$$

Czarnecki's discarded power is (Bitoleanu A., M. Popescu 2000)

$$D_C = \frac{P}{\cos \varphi_1} \times \\ \sqrt{FDI^2 - \sin^2 \varphi_1 \sum_{k=2}^{\infty} \frac{I_k}{I_1} \frac{\sin \varphi_k}{\sin \varphi_1} \left( 2 + \sum_{k=2}^{\infty} \frac{I_k}{I_1} \frac{\sin \varphi_k}{\sin \varphi_1} \right)}$$

For the active power imposed, these relations show the followings:

- the apparent power can be minimized if  $\cos \varphi_1 = 1$  and  $FDI=0$ ; this situation corresponds to the sinusoidal regime for voltage and current;
- Budeanu's reactive power depends only on the fundamental displacement factor;
- Budeanu's distortion power depends on the fundamental displacement factor and, also, on the current distortion factor;
- Czarnecki's reactive power depends on the displacement current angles of all the harmonics;
- Czarnecki's discarded power depends on the displacement current angles of all the harmonics and on the current distortion factor;
- because  $\cos \varphi_1$  and  $FDI$  depend on the structure of the filter, this requires detailed studies of the influence of the filter.

3.2. The Functioning Equations of the Transformer-Rectifier-Filter System

The functioning equations of the transformer-rectifier-filter system (fig. 1) in relative units, per phase, are (Bitoleanu A., M. Popescu 2001):

$$(11) u_1 = r_1 i_1 + l_{s1} \frac{di_1}{dt} - e_1$$

$$(12) e_1 = -l_m \frac{d(i_1 + i_2)}{dt} = e_2$$

$$(13) e_2 = r_2 i_2 + l_{s2} \frac{di_2}{dt} + u_2$$

$$(14) u_d = r i_r + l \frac{di_r}{dt} + u_c$$

$$(15) u_c = \frac{1}{C} \int_0^{\tau} (i_r - i_d) dt$$

$$(16) u_d = \begin{cases} |u_2| & \text{si } i_r \geq 0 \\ |u_c| & \text{si } i_r = 0 \end{cases}$$

$$(17) i_r \geq 0$$

$$(18) i_2 = \begin{cases} i_r & \text{if } e_2 \geq 0 \\ -i_r & \text{if } e_2 < 0 \end{cases}$$

The basic variables used in obtaining the relative units are:

$$(9) U_B = \sqrt{2}U_s \text{ - for the voltage; } I_B = I_{dN} \text{ (the average nominal value of the current) - for the current;}$$

$R_B = \frac{U_B}{I_B}$  - for the resistance;  $L_B = \frac{\sqrt{2}U_s}{\omega I_B}$  - for the

inductance;  $C_B = \frac{1}{\omega^2 L_B}$  - for the capacitance and

$T_B = \frac{1}{\omega}$  - for the time.

The equations (16), (17) and (18) are determined by the unilateral conduction of the rectifier and, so, it is impossible to analytically resolve the system. The Simulink program under Matlab offers remarkable facilities and allows the calculation of all the necessary characteristics for a complete power analysis. The Simulink model is obtained by the equations system.

### 3.3. The Current and Voltage Waveforms

The obtained model allows the visualisation of all the characteristics describing the functioning of the entire system for any combination of the values of the inductivity and the capacity in the DC link circuit. The variations in time of the rectified current and rectified voltage (fig.3 and 4) show that:

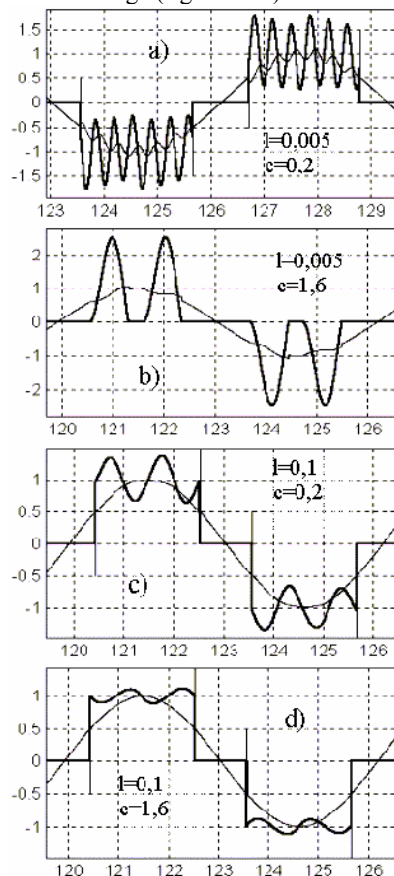


Fig. 3 The waveforms of the current and the voltage, in the transformer secondary, for different values of the filter, for single-phase bridge rectifier.

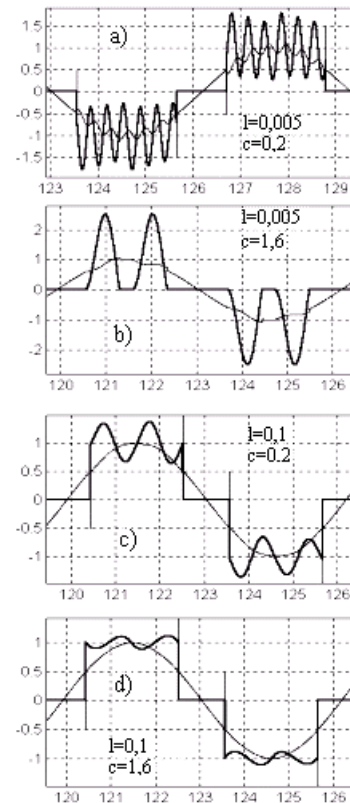


Fig. 4 The waveforms of the current and the voltage, in the transformer secondary, for different values of the filter, for three phase bridge rectifier

- the rectifier usually works in interrupted current regime; for three-phase bridge rectifier, the interrupted current regime can be avoided only for high values of the capacity and inductivity;

- the waveform of the rectifier output current is so that its average value is constant and equals the one of the inverter input current, because the average value of the capacity current is zero.

### 3.4. The total power factor

The power analysis offers supplementary reasons regarding the dimensioning of the filter and allows the complete characterisation of the functioning. As we are about to prove, considering exclusively the pulsation is insufficient and uneconomical (Popescu, M., A. Bitoleanu 2001).

#### The case of the supply from a single-phase bridge rectifier

The global power factor has the most interesting variation, implying special practical facts. So, it reaches a maximum value as a function of the capacity but only for low values of both the inductivity (beneath 0.02) and the capacity (fig.5a). As both the inductivity and the capacity have to be

higher (to limit pulsation), practically we can consider that the global power factor diminishes with the capacity. As function of the inductivity, the global power factor reaches always a maximum value (fig. 5b). This maximum value gets higher as the capacity gets lower and it corresponds to higher values of the inductivity, as the capacity gets lower. For all the values of the capacity, the global power factor diminishes rapidly when the inductivity becomes lower than the value corresponding to the maximum point, and diminishes slowly, when the inductivity becomes higher than this value. The power implications are immediate and important, consisting in the possibility of dimensioning the filter so that the power factor is maxim.

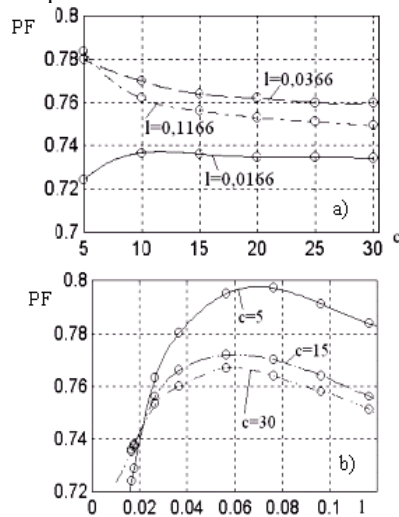


Fig. 5 The dependency of PF for single-phase bridge rectifier: a) – upon the relative capacity, for three different values of the inductivity; b) – upon the relative inductivity, for three different values of the capacity

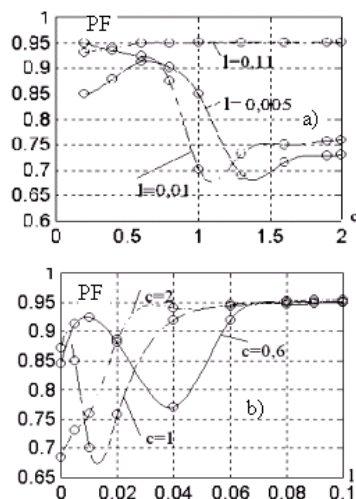


Fig. 6 The dependency of PF for three-phase bridge rectifier: a) – upon the relative capacity, for three different values of the inductivity; b) – upon the relative

This can be done using the dependency of the maximum power factor of the optimal inductivity and of the inverter voltage pulsation upon the relative capacity (fig. 6).

*The case of the supply from three-phase bridge rectifier*

In this case, for lower values of capacity and inductivity, the TPF variations (fig. 6) are significant. For medium values of capacity and inductivity and for high values of the capacity or the inductivity, the TPF is practically constant and high. This aspect shows that increasing the capacity and the inductivity up to certain values is not useful. The variations at the fig. 7 can be used for filter dimensioning.

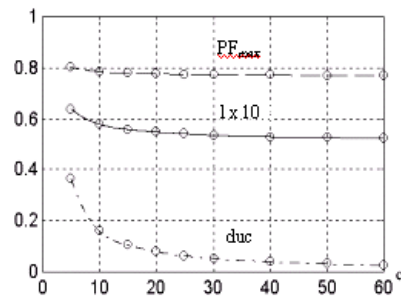


Fig. 7 The dependency of the maximum power factor, of the optimal inductivity and of the inverter voltage pulsations upon the relative capacity

The relation (6) can be used for TPF calculus. So, the errors between the TPF calculated by the relation (6) and obtained by simulation are smaller than 2,5 % (fig. 8). For high inductivity the errors are smaller than 1,5%.

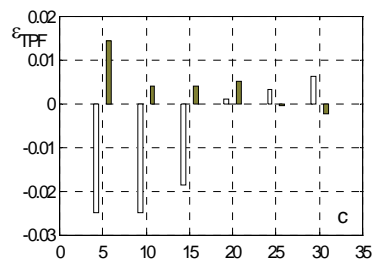


Fig. 8 The errors dependence of power factor using relation (6) and obtained by simulation versus capacity, for two values of inductivity

3.5. The experimental results

The experimental measurements have been obtained with a network analyzer Fluke 44b for a voltage converter with single-phase bridge rectifier, for two values of capacity and inductivity. The Fluke analyzer can measure the first 31 harmonics. The

measured values are lower, but the errors are smaller than 2,5 % (fig. 9).

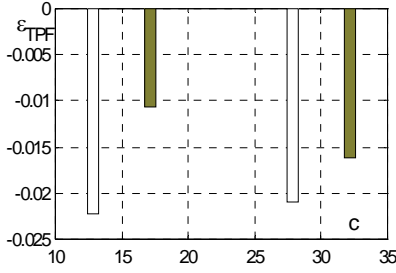


Fig. 9 The dependence of the errors of the experimental and simulated power factor on the capacity, for two values of the inductivity

### 3.6. Conclusions

The relations presented, show the direct dependence of the powers in un-sinusoidal regime and the fundamental displacement factor, on the current distortion factor and on the voltage distortion factor.

The filter in the DC circuit of a voltage and frequency static converter should contain an inductivity whose role doesn't consist only in limiting the pulsation of the current supplied by the rectifier. The filter affects the waveform of the current, and an unfit dimensioning could reduce the power performances of the converter. The right dimensioning of the filter is the best solution from the point of view of the power optimisation and it certainly satisfies the filtration requirements.

## 4. THE LINK BETWEEN THE STATIC CONVERTER AND THE ELECTRIC MOTOR

### 4.1. The mathematical characterization

In this case, the voltage and the current are un-sinusoidal

$$(19) u(t) = \sqrt{2} \sum_{k=1}^{\infty} U_k \sin(k\omega t - \varphi_{uk}),$$

$$i(t) = \sqrt{2} \sum_{k=1}^{\infty} I_k \sin(k\omega t - \varphi_{ik}).$$

The active power will be

$$(20) P = \sum_{k=1}^{\infty} U_k I_k \cos \varphi_k,$$

with  $\varphi_k = \varphi_{uk} - \varphi_{ik}$ .

he apparent power has the form

$$(21) S = \sqrt{\sum_{k=1}^{\infty} U_k^2} \sqrt{\sum_{k=1}^{\infty} I_k^2} = U_1 I_1 \sqrt{1 + FDU^2} \times \sqrt{1 + FDI^2}$$

or,

$$(22) S = \frac{P_1}{\cos \varphi_1} \sqrt{1 + FDU^2} \sqrt{1 + FDI^2} = \frac{1}{\cos \varphi_1} \left( P - \sum_{k=2}^{\infty} U_k I_k \cos \varphi_k \right) \times \sqrt{1 + FDU^2} \sqrt{1 + FDI^2}$$

The reactive and distortion powers of Budeanu and of Czarnecki have the general expressions and they are complicated and can't offer another conclusions.

It is interesting to study the minimization possibilities of the apparent power. So, if the fundamental active power is constant, the partial derivates of the apparent power in relation with  $\cos \varphi_1$ , FDI and FDU, are:

$$(23) \frac{\partial S}{\partial \cos \varphi_1} = - \frac{P_1}{\cos^2 \varphi_1} \sqrt{1 + FDU^2} \times \sqrt{1 + FDI^2} < 0$$

$$(24) \frac{\partial S}{\partial FDI} = \frac{P_1}{\cos \varphi_1} \sqrt{1 + FDU^2} \times \frac{FDI}{\sqrt{1 + FDI^2}} > 0$$

These expressions show that the apparent power has a minimum value when  $\cos \varphi_1 = 1$ , and FDI, FDU are zero. But, the active power is transmitted on all the harmonics and therefore this case ( $P_1 = \text{constant}$ ), is theoretically. If the total active power is constant, the partial derivate of the apparent power in relation with  $\cos \varphi_1$  is

$$(25) \frac{\partial S}{\partial \cos \varphi_1} = - \frac{1}{\cos^2 \varphi_1} \left( P - \sum_{k=2}^{\infty} U_k I_k \cos \varphi_k \right) \times \sqrt{1 + FDU^2} \sqrt{1 + FDI^2}$$

This expression isn't zero and it is negative. Therefore the minimum value of the apparent power is obtained for  $\cos \varphi_1 = 1$ . The partial derivates of the apparent power in relation with  $I_k$ ,  $k=2, \infty$  are:

$$\frac{\partial S}{\partial I_k} = - \frac{1}{\cos \varphi_1} U_k \cos \varphi_k \sqrt{1 + FDU^2} \sqrt{1 + FDI^2} + \frac{1}{\cos \varphi_1} \left( P - \sum_{k=2}^{\infty} U_k I_k \cos \varphi_k \right) \frac{\sqrt{1 + FDU^2}}{\sqrt{1 + FDI^2}} \frac{I_k}{I_1^2}$$

These expressions can be zero, when

$$(26) \quad U_k (1 + FDI^2) \cos \varphi_k = \left( P - \sum_{k=2}^{\infty} U_k I_k \cos \varphi_k \right) \frac{I_k}{I_1^2}$$

It is clearly that the equation has the solution  $I_k=0$ , only if  $\cos \varphi_k = 0$ . Generally, these equations have un-zero solutions. So, the (26) expression can be written in the following form:

$$(27) \quad \frac{U_k \cos \varphi_k}{U_1 \cos \varphi_1} \left( \frac{I_k}{I_1} \right)^2 - \frac{I_k}{I_1} + \frac{U_k \cos \varphi_k}{U_1 \cos \varphi_1} \times \left[ 1 + \sum_{j=2; j \neq k}^{\infty} \left( \frac{I_j}{I_1} \right)^2 \right] = 0$$

From (27) we obtain the  $(I_k/I_1)^2$  relations

$$(28) \quad \left( \frac{I_k}{I_1} \right)^2 = \frac{I_k}{I_1} \frac{U_1 \cos \varphi_1}{U_k \cos \varphi_k} - 1 - \left( \frac{I_2}{I_1} \right)^2 - \left( \frac{I_3}{I_1} \right)^2 - \dots - \left( \frac{I_{q-1}}{I_1} \right)^2 - \left( \frac{I_q}{I_1} \right)^2 - \left( \frac{I_{q+1}}{I_1} \right)^2 - \dots - \left( \frac{I_{k-1}}{I_1} \right)^2 - \left( \frac{I_{k+1}}{I_1} \right)^2 - \left( \frac{I_{k+2}}{I_1} \right)^2 \dots$$

and replace it in the some relation for  $q$  harmonic, after processing, result that (Popescu, M. 2001).

$$(29) \quad \frac{U_k \cos \varphi_k}{I_k} = \frac{U_q \cos \varphi_q}{I_q}, \quad \forall k, q \geq 2 \quad k \neq q$$

Introducing the impedances  $Z_k$  and  $Z_q$  corresponding of those both harmonics, the relation (30) can be writing after the form

$$(30) \quad \operatorname{Re}\{Z_k\} = \operatorname{Re}\{Z_q\}, \quad \forall k, q \geq 2 \quad k \neq q$$

#### 4.2. The asynchronous motor case

For asynchronous motor, with equivalence T scheme and ignoring iron losses, to obtain the equivalence impedance expression on the  $v$  harmonic

$$(31) \quad \underline{Z}_v = R_1 + \frac{R_2}{s_v} \frac{X_{mv}^2}{\left( \frac{R_2}{s_v} \right)^2 + (X_{\sigma v} + X_{mv})^2} + j \left[ X_{\sigma v} + X_{mv} \frac{\left( \frac{R_2}{s_v} \right)^2 + X_{\sigma v} (X_{\sigma v} + X_{mv})}{\left( \frac{R_2}{s_v} \right)^2 + (X_{\sigma v} + X_{mv})^2} \right]$$

where:

$R_1, R_2$  - the resistances on the phases of stator and rotor;

$X_{mv} = \omega_1 L_m$  - the magnetization reactance on the  $v$  harmonic;

$X_{\sigma v} = \omega_1 L_{\sigma}$  - the dispersion reactance of stator on the  $v$  harmonic ;

$X_{\sigma v} = \omega_1 L_{\sigma}$  - the dispersion reactance of rotor on the  $v$  harmonic ;

$s_v$  - the sleep on the  $v$  harmonic.

The real part of the impedance is

$$(32) \quad \operatorname{Re}\{\underline{Z}_v\} = R_1 + \frac{R_2}{s_v} \frac{X_{mv}^2}{\left( \frac{R_2}{s_v} \right)^2 + (X_{\sigma v} + X_{mv})^2}$$

and the sleep on the  $v$  harmonic has the expression

$$(33) \quad s_v = \frac{v-1+s}{v}$$

If we note with  $x$  the relative speed (reported to the synchronizing speed of the fundamental),  $x = p\omega / \omega_1$ , the sleep on the  $v$

harmonic to write  $s_v = \frac{v-x}{v}$ . So, the real part of the impedance will be:

$$(34) \quad \operatorname{Re}\{\underline{Z}_v\} = R_1 + \frac{v(v-x)R_2\omega_1^2 L_m^2}{(R_2)^2 + (v-x)^2 \omega_1^2 L_r^2}$$

where  $L_r$  is the total rotor inductivity,  $L_r = L_m + L_{\sigma r}$ .

It is clearly that the real part of the impedances is depended of the order of harmonics and it can't be constant. The dependencies of the real part of the impedance versus sleep show followings (Fig. 10):

- at lower frequencies ( $f < 2,5$  Hz), the real parts of the impedances are different;
- after these frequencies there is a sleep for which the real parts of the impedances are practically equal;
- these sleeps there are nearly unit when the frequency increase and can't be an optimum solutions physic point of view. So, it result there aren't an optimum solution that minimize the apparent power at constant active power. In practice obtaining a working point ( $\omega, M$ ), is more important and study optimization of this case can be more interesting. This optimization problem is complicate and can't be resolved on the analytic way.

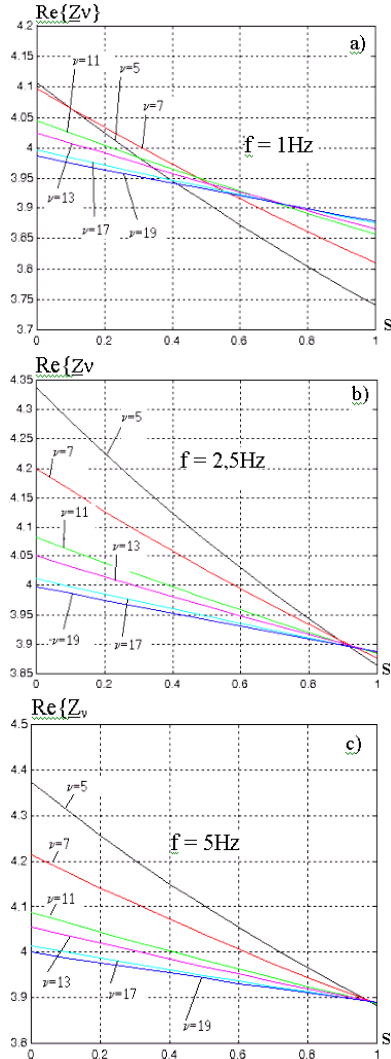


Fig. 10 The dependencies of real parts of equivalence impedances for first 19 harmonics, versus the sleep, at different frequencies

#### 4.3. The supply asynchronous motor from amplitude modulation voltage inverter

If the asynchronous motor is supplied from amplitude modulation voltage inverter, the phase voltage spectrum is (Popescu, M. 2001)

$$(31) U_v = \frac{4\sqrt{2}}{3\pi v} U_d \sin v \frac{\pi}{3} \sin v \frac{\pi}{2} \cos v \frac{\pi}{6}.$$

Numerical resolving of minimization apparent power at constant mechanical power optimization problem is successfully. Really, there are optimum values of voltage and frequency that minimize the apparent power. The graphical representation of apparent power versus frequency at constant mechanical power shows this (fig. 11).

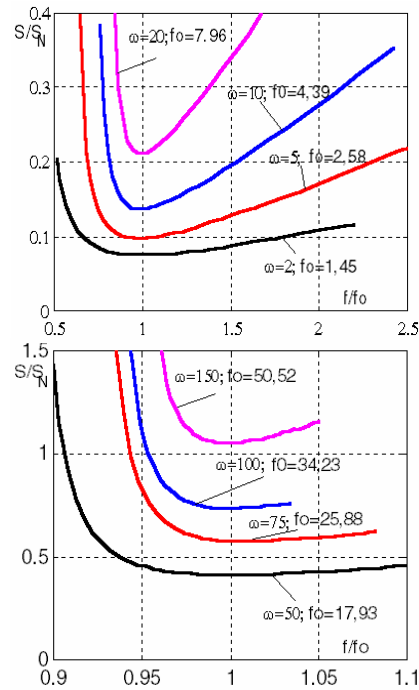


Fig. 11 The relative units dependencies of apparent power versus relative frequency for diferent speeds, at nominal torque

The results corresponding to the motor with following dates:  $P_N=2,6kW$ ,  $U_N=380V$ ,  $I_N=6A$ ,  $n_N=1442rot/min$ ,  $R_1 = 1,61\Omega$ ,  $R_2 = 1,52\Omega$ ,  $L_{\sigma}=0,0085H$ ,  $L_{\sigma r}=0,012H$ ,  $L_m=0,2456H$ .

It is significantly that the apparent power variations are bigger at lower frequencies given optimum value. So, if the frequency is lower with 0,5 Hz, the apparent power increase with 20%. Also, the optimum values of apparent power increase if the speed increases.

It is very important that the dependence of optimum values of effective voltage versus optimum frequencies is linearly (fig. 12). So, optimum control implementation is easy. Also, comparative with the  $V/f=V_N/f_N$  control, the optimum values of voltage are higher until half nominal

#### 4.4. Experimental results

The experimental determinations were done in the following conditions:

- we used a voltage inverter with BPT ( $V_{CE} = 600V$ ,  $I_C = 30 A$ ) supplied from controlled mono-phase rectifier;
- the asynchronous motor used was taken above;
- for a speed fixed and ten values of frequency, the d.c. voltage was regulated until the nominal torque was obtained.

These results confirm numerical calculus completely. So, the relative apparent power dependencies versus frequency are very nearly (fig. 13), and errors between the optimum frequencies calculated and experimentally ascertained are less than 3%.

#### 4.4. Conclusions

The relations found by the authors show direct dependence through the powers in un-sinusoidal regime and the fundamental displacement factor, the current distortion factor and the voltage distortion factor. It is very important that there is an optimal control voltage – frequency that minimizes apparent power. The optimum voltage – frequency dependence is linearly and optimum control implementation is easy.

#### 5. REFERENCES

- Bitoleanu, A., M. Popescu (1998). Energetical Analysis of the Electrical Drive with Induction Motor and Voltage Source Frequency Converter. In: *8<sup>th</sup> International Power Electronics & Motion Control Conference*, September 8-10, 1998, Prague, the Czech Republic, pg. 6/108-6/112.
- Bitoleanu A., M. Popescu (1999). The energetical Interaction of the Electrical Drive with Induction Motor and Harmonics Elimination Voltage Source Converter with the Network In: *3rd International Symposium on Advanced Electromechanical Motion Systems* Patras, July 8-9, 1999,.
- Bitoleanu A., M. Popescu (2000). Energetical Aspects of the Voltage and Frequency Static Converter with Asynchronous Motor Driving Systems. In: *Buletinul Institutului Politehnic din Iasi, Tomul XLVI (L), Fasc. 5, 2000.*
- Bitoleanu A., M. Popescu (2001). Energetical optimization of the dc link circuit in the static converter and ac motors. In: *ACEMP 2001*, 27-29 June 2001, Kuşadası Turkey, pg. 171-176.
- Budeanu C.I. (1936). Sur le transfert des phénomènes déformants. In : *C.R. de l'Acad. des Sciences de Paris*, 27 janvier (1936).
- Czarnecki L.S. (1985). Considerations of the reactive powers in nonsinusoidal situations. In: *IEEE Trans. on Instrumentat. and Meas.* IM-34, 399-404.
- Czarnecki L.S. (1992). Distortion power in systems with nonsinusoidal voltage. In: *IEE Proceedings-B, Vol.139*, No.3, May.
- Popescu, M. (2001). Aspecte energetice ale sistemelor de acționare cu motoare asincrone și convertoare statice indirecte de tensiune și frecvență. *Teză de doctorat*, Universitatea din Craiova.
- Popescu, M., A. Bitoleanu (2001). Comparative Analysis of the Energetical Impact of the Electrical Drive with Induction Motor and Voltage Source Converter on the Network, *Electromotion*, nr. 4/2001.